

Phase space analysis of $f(Q)$ gravity accelerating cosmological models

S.A. Narawade^{1,*} Shashank P. Singh^{1,†} and B. Mishra^{1,‡}

¹*Department of Mathematics, Birla Institute of Technology and Science-Pilani, Hyderabad Campus, Hyderabad-500078, India.*

Abstract: The dynamical aspect of accelerating cosmological model has been studied in this paper in the context of modified symmetric teleparallel gravity, the $f(Q)$ gravity. Initially, we have derived the dynamical parameters for two well known form of $f(Q)$ such as: (i) log-square-root form and (ii) exponential form. The equation of state (EoS) parameter for the dark energy in the $f(Q)$ gravity in both the models emerges into a dynamical quantity. At present both the models show the quintessence behavior and behave like the Λ CDM at the late time. Further, the dynamical system analysis has been performed to determine the cosmological behaviour of the models along with its stability behaviour. For both the models the critical points are obtained and analysed the stability at each critical points with phase portraits. The evolutionary behaviour of density parameters for the matter-dominated, radiation-dominated, and dark energy phases are also shown for both the models.

Keywords: Symmetric teleparallel gravity, Hybrid scale factor, Phase space analysis.

I. INTRODUCTION

One of the most important implications of the equivalence principle is the expression of gravity through space-time curvature. The most successful theory to explain gravitational interaction is Einstein's general theory of relativity (GR), and the Λ CDM(Cold Dark Matter) hypothesis is the concordance cosmological model based on GR. The non-renormalizability GR, the cosmological constant problem, the coincidence problem, the Hubble tension, the σ_8 tension, etc. are some of the theoretical and observational issues that this basic gravitational and cosmological framework faces [1–7]. After astronomical observations of Supernovae over the past few decades [8, 9], a number of ideas have been proposed to modify the GR and take into account various formulations of gravity. Depending on the choice of connection, one can classify the theories of gravity into three classes: (i) The first one involves use of GR, free torsion, and metric-compatible connections; (ii) The second class, torsion is connected using a metric-compatible, curvature-free approach, such as the teleparallel GR equivalent [10]; and (iii) finally the symmetric teleparallel equivalent of GR, requires a curvature and torsion-free connection that is not metrically compatible [11]. These three equivalent formulations based on the three different connections are commonly known as The Geometrical Trinity of Gravity [12]. In spite of the fact that these three theories are similar at the level of field equations, however, their modifications could not be comparable at the fundamental level [13].

The cosmological and astrophysical implications of symmetric teleparallel gravity developed into coincident GR or $f(Q)$ gravity [14], are being given significance in recent literature on extended theories of gravity. Various work in the literature suggest that the $f(Q)$ theory is one of the promising alternative formulations of gravity to explain cosmological observations [15–19]. Soudi et al. shows that gravitational wave polarizations have a significant role in restricting the strong field behavior of the gravitational theories [20]. Harko et al. have explored an extension of the symmetric teleparallel gravity, by considering a new class of theories where the non-metricity Q is coupled non-minimally to the matter Lagrangian, in the framework of the metric-affine formalism. As in the standard curvature-matter couplings, this nonminimal Q -matter coupling entails the non-conservation of the energy-momentum tensor, and consequently the appearance of an extra force [21]. Testing against a variety of current cosmological observation data, including Type Ia Supernovae, Pantheon data, Hubble data, etc., has been done in order to place observational constraints on the background behaviour of several $f(Q)$ models [22–24]. The motivation behind the $f(Q)$ gravity is to modify the gravitational interactions in such a way that the late time cosmic phenomena can be well explained. The theory allows additional degrees of freedom beyond that of GR, so that it

* shubhamn2616@gmail.com

† shashanksingh23101@gmail.com

‡ bivu@hyderabad.bits-pilani.ac.in

can lead to new gravitational interactions. In the literature, one can find some research [25–31] on this gravitational theory, but its limitations and predictions are yet to be investigated, in particular its ability to address the cosmic acceleration issue.

Before we consider this gravity as a viable alternative to GR, another crucial issue of $f(Q)$ gravity to be addressed, i.e the stability of its cosmological models. One among several stability analysis is the dynamical stability analysis [32] that studies the behavior of a model under small perturbations. To be specific, it aims at to find the model coming back to the original state or evolve into a different solution. This analysis further provides an accurate prediction on the behaviour of the model pertaining to the physical scenario and thereby resulted in a robust theoretical framework. One can refer some papers on dynamical system analysis in modified theories of gravity [33–40].

The form of the function $f(Q)$ defined in this gravity has a major role on the behaviour of the model. The motivation here is to appropriately choose some physically viable form of $f(Q)$ to address the issue of cosmic acceleration and further to check the robustness of the model by performing the dynamical stability analysis. The result may provide some crucial insights into the viability of $f(Q)$ gravity and its possible contribution to understanding of the structure and evolution of the Universe. The paper is organised as follows: In Sec. II, the formulation of $f(Q)$ gravity as well its field equations are presented. In Sec. III, two cosmological models are given with some well defined form of $f(Q)$. The dynamical system analysis has been performed in Sec. IV to obtain the critical points and its behaviour. The results and conclusions are noted in Sec. V.

II. FIELD EQUATIONS OF $f(Q)$ GRAVITY

We will briefly discuss the $f(Q)$ gravity and its derivation to obtain the field equations. The action of $f(Q)$ gravity [28],

$$S = \int \frac{1}{2} [Q + f(Q)] \sqrt{-g} d^4x + \int \mathcal{L}_m \sqrt{-g} d^4x, \quad (1)$$

where g denotes the determinant of the metric tensor ($g_{\mu\nu}$) and \mathcal{L}_m denotes the matter Lagrangian. The covariant derivative of the metric tensor is the non-metricity tensor, which can be expressed as,

$$Q_{\alpha\mu\nu} = \nabla_\alpha g_{\mu\nu} = \frac{\partial g_{\mu\nu}}{\partial x^\beta} \quad (2)$$

and the two traces are,

$$Q_\alpha = Q_\alpha^\mu{}_\mu \quad \text{and} \quad \tilde{Q}^\alpha = Q_\mu{}^{\alpha\mu}. \quad (3)$$

The general affine connection can be decomposed into Levi-Civita connection [41, 42] $\left(\left\{{}^\lambda{}_{\mu\nu}\right\}\right)$, contortion $\left(K^\lambda{}_{\mu\nu}\right)$ and disformation $\left(L^\lambda{}_{\mu\nu}\right)$ as,

$$\Gamma^\lambda{}_{\mu\nu} = \left\{{}^\lambda{}_{\mu\nu}\right\} + K^\lambda{}_{\mu\nu} + L^\lambda{}_{\mu\nu}, \quad (4)$$

where

$$\left\{{}^\lambda{}_{\mu\nu}\right\} = \frac{1}{2} g^{\lambda\alpha} \left(\partial_\mu g_{\alpha\nu} + \partial_\nu g_{\alpha\mu} - \partial_\alpha g_{\mu\nu} \right), \quad K^\lambda{}_{\mu\nu} = \frac{1}{2} \left(T^\lambda{}_{\mu\nu} + T_\mu{}^\lambda{}_\nu + T_\nu{}^\lambda{}_\mu \right),$$

$$L^\lambda{}_{\mu\nu} = \frac{1}{2} \left(Q^\lambda{}_{\mu\nu} - Q_\mu{}^\lambda{}_\nu - Q_\nu{}^\lambda{}_\mu \right), \quad T^\lambda{}_{\mu\nu} = \Gamma^\lambda{}_{\mu\nu} - \Gamma^\lambda{}_{\nu\mu}.$$

The superpotential of the Model-I is

$$P_{\mu\nu}^\alpha \equiv -\frac{1}{4}Q_{\mu\nu}^\alpha + \frac{1}{4}\left(Q_{\mu}^{\alpha\nu} + Q_{\nu}^{\alpha\mu}\right) + \frac{1}{4}Q^\alpha g_{\mu\nu} - \frac{1}{8}\left(2\tilde{Q}^\alpha g_{\mu\nu} + \delta_\mu^\alpha Q_\nu + \delta_\nu^\alpha Q_\mu\right). \quad (5)$$

The energy momentum tensor is,

$$T_{\mu\nu} = -\frac{2}{\sqrt{-g}}\frac{\delta\sqrt{-g}\mathcal{L}_m}{\delta g^{\mu\nu}} \quad (6)$$

Varying action (1) with respect to the metric tensor, we can get the field equations of $f(Q)$ gravity as [28],

$$\frac{2}{\sqrt{-g}}\nabla_\alpha\left(\sqrt{-g}P_{\mu\nu}^\alpha + \sqrt{-g}f_Q P_{\mu\nu}^\alpha\right) + \frac{g_{\mu\nu}}{2}(Q + f(Q)) + (1 + f_Q)\left(P_{\mu\alpha\beta}Q_\nu^{\alpha\beta} - 2Q_{\alpha\beta\mu}P_\nu^{\alpha\beta}\right) = -T_{\mu\nu}, \quad (7)$$

where f_Q be the derivative of $f(Q)$ in non-metricity scalar and $Q = 6H^2$ with H be the Hubble parameter. Now, to frame the cosmological model, we consider the FLRW space time,

$$ds^2 = -dt^2 + a(t)(dx^2 + dy^2 + dz^2) \quad (8)$$

where $a(t)$ represents the scale factor and the energy momentum tensor in the form of perfect fluid as,

$$T_{\mu\nu} = (\rho + p)u_\mu u_\nu + pg_{\mu\nu}, \quad (9)$$

where p, ρ respectively be the pressure and energy density. Now, the field equations of $f(Q)$ gravity in perfect fluid can be obtained as [28],

$$\rho = \frac{1}{2}(Q + 2Qf_Q - f), \quad (10)$$

$$p = \frac{1}{2}(f - Q - 2Qf_Q) - 2\dot{H}(2Qf_{QQ} + f_Q + 1). \quad (11)$$

We denote $f(Q) = f$ and $f_Q = \frac{\partial f}{\partial Q}$ and also we consider that the Universe is filled with dust and radiation fluids. Hence,

$$\rho = \rho_m + \rho_r; \quad p = \frac{1}{3}p_r$$

with ρ_m and ρ_r represents the energy density for the dust and radiation fluid respectively. Then from Eqns. (10) and (11), we get

$$\rho_{eff} = 3H^2 = \rho_r + \rho_m + \rho_{de}, \quad (12)$$

$$-p_{eff} = 2\dot{H} + 3H^2 = -p_r - p_m - p_{de}, \quad (13)$$

where p_m, p_r respectively denotes the pressure of matter and radiation phase; ρ_{de} and p_{de} be the energy density and pressure of dark energy phase, which can be expressed as,

$$\begin{aligned} \rho_{de} &= \frac{f}{2} - Qf_Q, \\ p_{de} &= 2\dot{H}(2Qf_{QQ} + f_Q) + Qf_Q - \frac{f}{2}. \end{aligned}$$

and the effective EoS parameter and EoS parameter due to dark energy are,

$$\omega_{eff} = \frac{p_{eff}}{\rho_{eff}} = -1 + \frac{\Omega_m + \frac{4}{3}\Omega_r}{2Qf_{QQ} + f_Q + 1}, \quad (14)$$

$$\omega_{de} = \frac{p_{de}}{\rho_{de}} = -1 + \frac{4\dot{H}(2Qf_{QQ} + f_Q)}{f - 2Qf_Q}. \quad (15)$$

The density parameter pertaining to pressure-less matter, radiation and dark energy respectively denoted as,

$$\Omega_m = \frac{\rho_m}{3H^2}, \quad \Omega_r = \frac{\rho_r}{3H^2}, \quad \Omega_{de} = \frac{\rho_{de}}{3H^2}. \quad (16)$$

The EoS parameter describes the present state of the Universe. A bunch of cosmological observations recently constrained the current value of the EoS parameter to be, $\omega_{eff} = -1.29^{+0.15}_{-0.12}$ [43], $\omega_{eff} = 1.3$ [44], Supernovae Cosmology Project, $\omega_{eff} = -1.035^{+0.055}_{-0.059}$ [45]; WAMP+CMB, $\omega_{eff} = -1.079^{+0.090}_{-0.089}$ [46]; Plank 2018, $\omega_{eff} = -1.03 \pm 0.03$ [47] or $\omega_{eff} = -1.33^{+0.31}_{-0.42}$ [48].

To solve the above system and to analyse the behaviour of the dynamical parameters, we consider some form of Hubble parameter H and the function $f(Q)$. The Hubble parameter, $H = \xi + \frac{\eta}{t}$ corresponds to the scale factor, $a(t) = e^{\xi t} t^\eta$, known as the hybrid scale factor [49–52]. Subsequently, the non-metricity scalar becomes, $Q = 6H^2 = 6 \left(\xi + \frac{\eta}{t} \right)^2$. This form of Hubble parameter further provides a time varying deceleration parameter $\left(q = -1 + \frac{\eta}{(\xi t + \eta)^2} \right)$, which can simulate a cosmic transition from early deceleration to late time acceleration. The deceleration parameter, $q \approx -1 + \frac{1}{\eta}$ when $t \rightarrow 0$ whereas $q \approx -1$ when $t \rightarrow \infty$. To realise the positive deceleration at early Universe for the transient Universe, the scale factor parameter η should be $0 < \eta < 1$. The transition can occur at $t = -\frac{\eta}{\xi} \pm \frac{\sqrt{\eta}}{\xi}$. We will restrict to the positivity of the second term and ignore the negativity. This is because the negativity of the second term would provide negative time, which may lead to unphysical situation at the bigbang scenario. In that case also the parameter η restricted to $0 < \eta < 1$, since the cosmic transit may have occurred at, $t = \frac{-\eta + \sqrt{\eta}}{\xi}$. The jerk parameter, $j = 1 - \frac{3\eta}{(\eta + \xi t)^2} + \frac{2\eta}{(\eta + \xi t)^3}$.

III. THE $f(Q)$ GRAVITY MODELS

A. Model-I

We first consider the logarithmic form of $f(Q)$ [53] as,

$$f(Q) = n Q_0 \sqrt{\frac{Q}{\lambda_1 Q_0}} \ln \frac{\lambda_1 Q_0}{Q}, \quad (17)$$

where n and $\lambda_1 > 0$ are free parameters; $Q_0 = 6H_0^2$, where H_0 represents the present value of H . For $n = 0$, one can recover the GR equivalent model.

At the outset, we have studied the evolutionary behaviour of the function $f(Q)$ by plotting the graphs $\frac{f(Q)}{H_0^2}$ vs $z + 1$ and f_Q vs $z + 1$ where z is redshift [29]. We wish to analyse $\frac{f(Q)}{H_0^2}$ and f_Q as functions of redshift since the Hubble parameter is related to the scale factor as $H = \frac{\dot{a}}{a}$. One can see from FIG.- 1 as time passes, $\frac{f(Q)}{H_0^2}$ shows a decreasing behavior and gradually vanishes. Similarly, f_Q starts with a high positive value, decreases over time, and remains positive throughout.

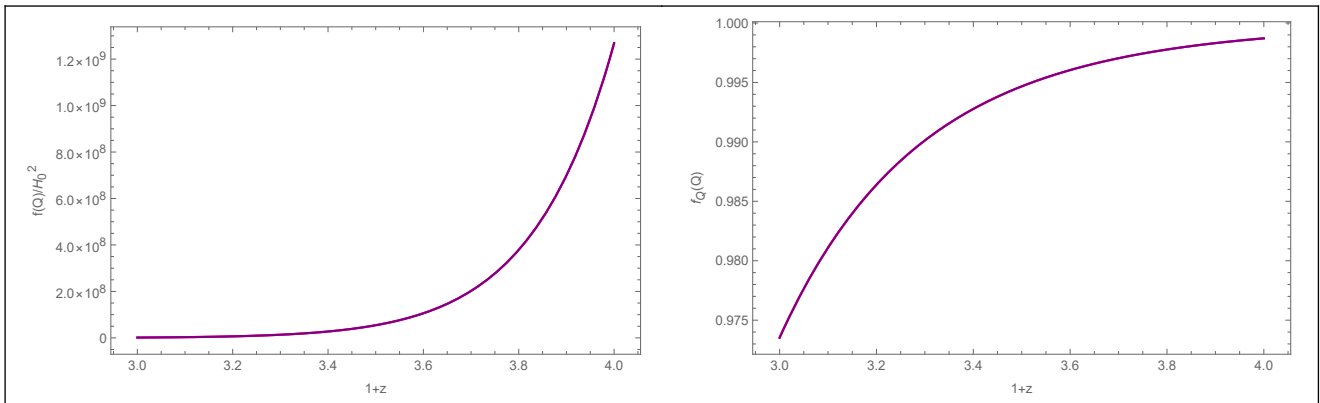


FIG. 1. Evolution of $\frac{f(Q)}{H_0^2}$ (Left Panel) and $f_Q(Q)$ (Right Panel) in $1+z$. The parameter scheme: $\xi = 0.965$, $\eta = 0.22$, $n = 1$, $Q_0 = 29990$ and $\lambda_1 = 0.35$.

Using Eqn. (17), Eqns. (10), (11) and (14) reduces to,

$$p_{eff} = \frac{\lambda_1 \Omega_r (z+1)^4 \sqrt{\frac{H^2(z)}{\lambda_1 Q_0}} - 3\sqrt{6}H^2(z)n + \sqrt{6}H(z)n(z+1)H_z(z)}{3\lambda_1 \sqrt{\frac{H^2(z)}{\lambda_1 Q_0}}}, \quad (18)$$

$$\rho_{eff} = H(z)Q_0n\sqrt{\frac{6}{\lambda_1 Q_0}} + \Omega_r(z+1)^4 + \Omega_m(z+1)^3, \quad (19)$$

$$\omega_{eff} = \frac{\lambda_1 \Omega_r (z+1)^4 \sqrt{\frac{H^2(z)}{\lambda_1 Q_0}} - 3\sqrt{6}H^2(z)n + \sqrt{6}H(z)n(z+1)H_z(z)}{3\sqrt{\frac{H^2(z)}{\lambda_1 Q_0}} \left(\sqrt{6}\lambda_1 Q_0 n \sqrt{\frac{H^2(z)}{\lambda_1 Q_0}} + \lambda_1(z+1)^3(\Omega_m + \Omega_r z + \Omega_r) \right)}. \quad (20)$$

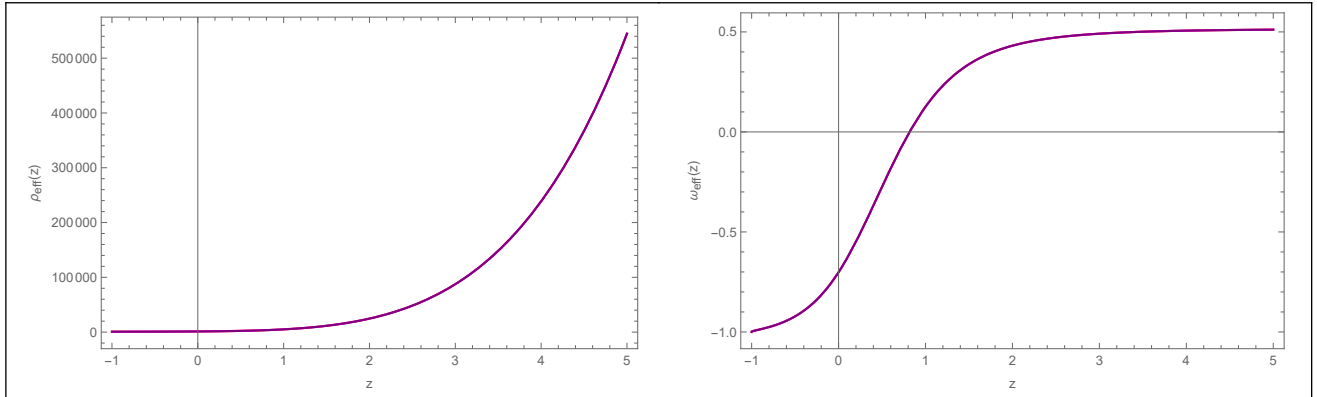


FIG. 2. Evolution of effective energy density (Left Panel) and effective EoS parameter (Right Panel) in redshift. The parameter scheme: $\xi = 0.965$, $\eta = 0.22$, $n = 1$, $Q_0 = 29990$, $\lambda_1 = 0.35$, $\Omega_m = 0.3$ and $\Omega_r = 0.00001$.

Where H_z denotes the $\frac{dH(z)}{dz}$. The parameters ξ , η , n , Q_0 and λ_1 determine the evolutionary behavior of effective energy density and effective EoS parameter. The model parameter has been constrained to obtain the positive energy density FIG.- 2 (Left Panel). The effective energy density is showing decreasing behavior from early epoch to late epoch and remains positive throughout. The effective EoS parameter shows quintessence behavior at present epoch, whereas it converges to Λ CDM in late epoch [FIG.- 2 (Right Panel)]. At $z = 0$, the value of effective EoS parameter observed to be ≈ -0.7013 .

B. Model-II

As a second model, we consider an exponential function of $f(Q)$ [27] as,

$$f(Q) = Q e^{\frac{\mu \lambda_2}{Q}} - Q, \quad (21)$$

where λ_2 is the free parameter. In the cosmological framework, the model gives rise to a scenario without Λ CDM as a limit, having the same number of free parameters as Λ CDM. In this model, in certain time period of cosmic history, the term $\frac{\mu}{Q}$ decreases, which ends up making the model as polynomial one.

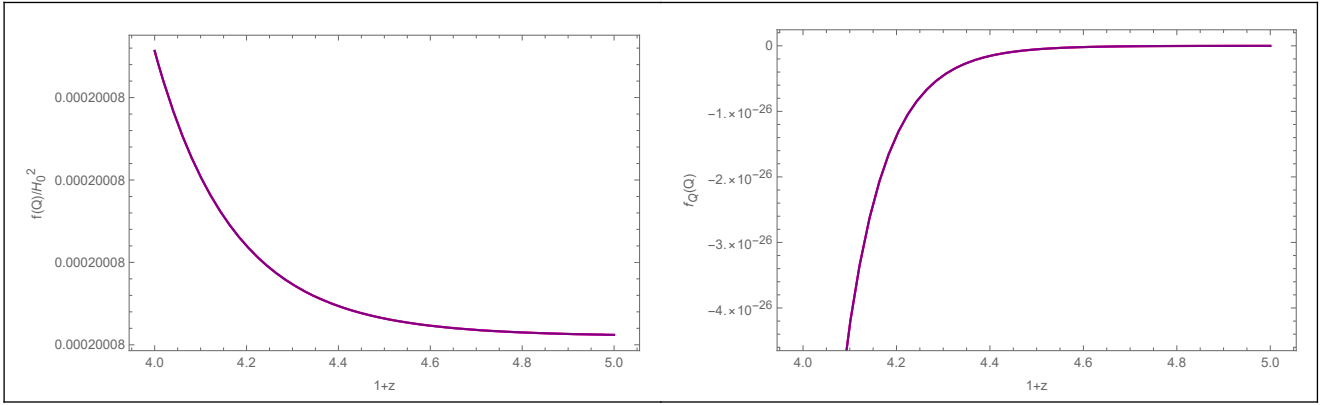


FIG. 3. Evolution of $\frac{f(Q)}{H_0^2}$ (Left Panel) and $f_Q(Q)$ (Right Panel) in $1+z$. The parameter scheme: $\xi = 0.965$, $\eta = 0.22$, $\mu = 2.5$ and $\lambda_2 = 6.5$

We can see the behaviour of $\frac{f(Q)}{H_0^2}$ and f_Q in FIG.- 3. In this model also, the normalized non-metricity function $\frac{f(Q)}{H_0^2}$ increases with cosmic time due to exponential form of model. However, the functional f_Q becomes a decreasing function of the redshift. The motivation behind these plots is that the non-metricity scalar Q at the FLRW background assumes $6H^2$. To analyse the dynamic behavior of the model, the dynamical parameters can be derived from Eqns. (10), (11) and (14) by incorporating Eqn. (21) as,

$$p_{eff} = -3H^2(z) + 2H(z)(z+1)H_z(z) - \frac{e^{\frac{\lambda_2\mu}{6H^2(z)}} (9H^3(z)(3H^2(z)+\lambda_2\mu)+\lambda_2\mu(z+1)H_z(z)(9H^2(z)+\lambda_2\mu))}{54H^5(z)} + \frac{1}{3}\Omega_r(z+1)^4, \quad (22)$$

$$\rho_{eff} = \frac{1}{6}e^{\frac{\lambda_2\mu}{6H^2(z)}} \left(\frac{\lambda_2\mu}{H^2(z)} + 3 \right) + 3H^2(z) + (z+1)^3(\Omega_m + \Omega_r z + \Omega_r), \quad (23)$$

$$\omega_{eff} = \frac{-3H^2(z) + 2H(z)(z+1)H_z(z) - \frac{e^{\frac{\lambda_2\mu}{6H^2(z)}} (9H^3(z)(3H^2(z)+\lambda_2\mu)+\lambda_2\mu(z+1)H_z(z)(9H^2(z)+\lambda_2\mu))}{54H^5(z)} + \frac{1}{3}\Omega_r(z+1)^4}{\frac{1}{6}e^{\frac{\lambda_2\mu}{6H^2(z)}} \left(\frac{\lambda_2\mu}{H^2(z)} + 3 \right) + 3H^2(z) + (z+1)^3(\Omega_m + \Omega_r z + \Omega_r)} \quad (24)$$

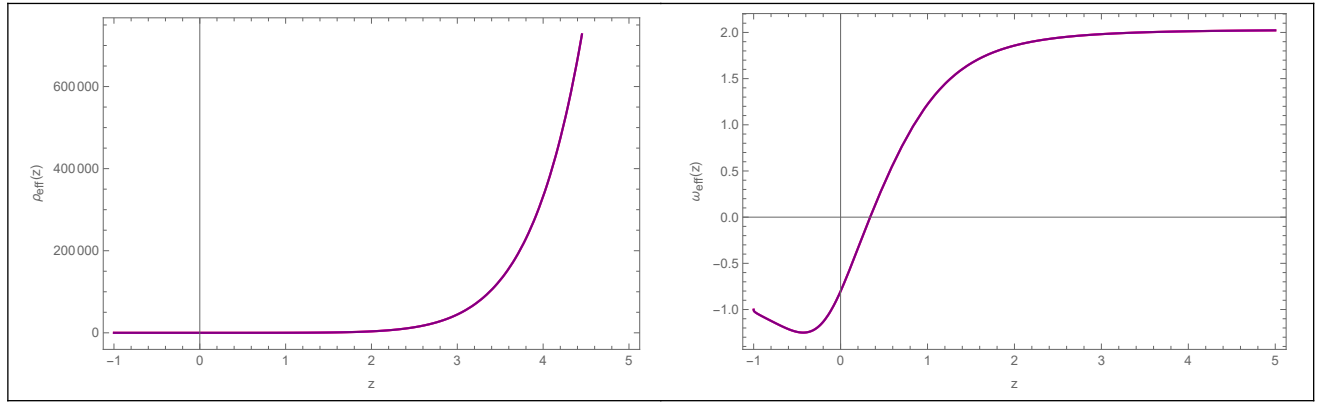


FIG. 4. Evolution of effective energy density (Left Panel) and effective EoS parameter (Right Panel) in redshift. The parameter scheme: $\xi = 0.965$, $\eta = 0.22$, $\mu = 2.5$, $\lambda_2 = 6.5$, $\Omega_m = 0.3$ and $\Omega_r = 0.00001$.

FIG.- 4 (Left Panel) shows the evolutionary behaviour of effective energy density, which is decreasing and vanishing at late time. The effective energy density remains positive throughout the evolution. The present value of

effective EoS parameter is $\omega_{eff} = -0.8024$ [FIG.- 4 (Right Panel)]. The effective EoS parameter gives quintessence behavior at present time, whereas it converges to Λ CDM at late time of the evolution.

IV. DYNAMICAL SYSTEM ANALYSIS

We shall perform the dynamical system analysis of the background equations of the two models and will focus on its stability [54, 55]. To do so, we consider 3-dimensionless parameters, x, y and σ , and transform the field equations in terms of the dynamical variables as,

$$x = \frac{f}{6H^2}, \quad y = -2f_Q, \quad \sigma = \frac{\rho_r}{3H^2}$$

Subsequently, Eqn. (16) reduces to,

$$\begin{aligned} \Omega_r &= \sigma, \\ \Omega_{de} &= x + y, \\ \Omega_m &= 1 - x - y - \sigma \\ \frac{\dot{H}}{H^2} &= \frac{-(3 - 3x - 3y + \sigma)}{2(2Qf_{QQ} + f_Q + 1)}. \end{aligned}$$

Here, prime (') represents differentiation with respect to the number of e-folds of the universe, $N = \ln a$, then we can differentiate x, y , and σ with respect to N , to get the following equations,

$$x' = \frac{(3 - 3x - 3y + \sigma)(2x + y)}{2(2Qf_{QQ} + f_Q + 1)}, \quad (25)$$

$$y' = (3 - 3x - 3y + \sigma) \left[1 + \frac{(y - 2)}{2(2Qf_{QQ} + f_Q + 1)} \right], \quad (26)$$

$$\sigma' = \sigma \left[\frac{(3 - 3x - 3y + \sigma)}{(2Qf_{QQ} + f_Q + 1)} - 4 \right]. \quad (27)$$

Now, we can redefine ω_{eff} and ω_{de} as

$$\begin{aligned} \omega_{eff} &= -1 - \frac{2}{3} \frac{\dot{H}}{H^2}, \\ \omega_{de} &= -1 - \frac{1}{3(x + y)} \left[y' + \frac{\dot{H}}{H^2} y \right]. \end{aligned}$$

For $f(Q) = nQ_0 \sqrt{\frac{Q}{\lambda_1 Q_0}} \ln(\frac{\lambda_1 Q_0}{Q})$ [Model-I], one can express Eqns. (25)-(27) in terms of dynamical variables as,

$$x' = \frac{(2x + y)(3 - 3x - 3y + \sigma)}{(2 - x - y)}, \quad (28)$$

$$y' = \frac{x(3x + 3y - 3 - \sigma)}{(2 - x - y)}, \quad (29)$$

$$\sigma' = \frac{2\sigma(\sigma - x - y - 1)}{(2 - x - y)}. \quad (30)$$

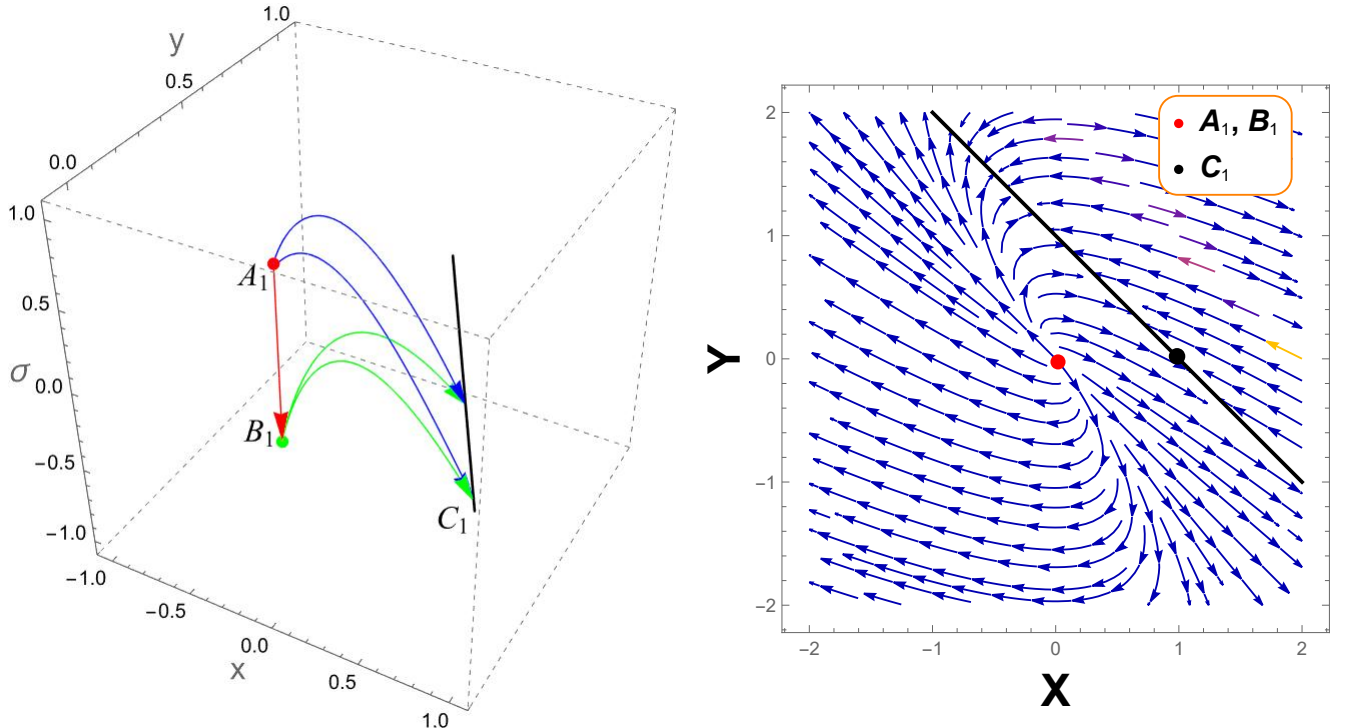
Moreover, the effective EoS parameter and EoS parameter for dark energy can be written in dynamical variables as,

$$\begin{aligned} \omega_{eff} &= -1 - \frac{2}{3} \left(\frac{3x + 3y - \sigma - 3}{2 - x - y} \right), \\ \omega_{de} &= -\frac{3 - \sigma}{3(2 - x - y)}. \end{aligned}$$

Name	Point/Curve	Ω_m	Ω_r	Ω_{de}	q	ω_{eff}	ω_{de}	Phase of Universe	Stability
A_1	$(0, 0, 1)$	0	1	0	1	$\frac{1}{3}$	$-\frac{1}{3}$	Radiation dominated	Unstable
B_1	$(0, 0, 0)$	1	0	0	$\frac{1}{2}$	0	$-\frac{1}{2}$	Matter dominated	Unstable
C_1	$(x, 1 - x, 0)$	0	0	1	-1	-1	-1	Dark energy dominated	Stable

TABLE I. Critical Points and the corresponding cosmology for Model-I

TABLE I provides the critical points and the cosmological behaviour at these points. The details description of each critical point has been narrated below. In FIG.- 5, the 2D and 3D phase portrait have been given to understand the stability of these points.

FIG. 5. Phase-space trajectories on the x - y - σ plane (Left Panel) and the portrait on the x - y plane (Right Panel) for Model-I.

- **Critical point $A_1 (0, 0, 1)$:** The corresponding EoS parameter and deceleration parameter is $\omega_{eff} = \frac{1}{3}$ and $q = 1$ respectively. This behaviour of the critical point leads to the decelerating phase of the Universe. Also, density parameters are $\Omega_{de} = 0$, $\Omega_m = 0$ and $\Omega_r = 1$. This critical point is an unstable node because it contains all positive eigenvalues of the Jacobian matrix,

$$\{2, 2, 1\}.$$

- **Critical Point $B_1 (0, 0, 0)$:** The critical point leads to the decelerating phase of the Universe, since the EoS parameter corresponding to this critical point is $\omega_{eff} = 0$ and deceleration parameter is $q = \frac{1}{2}$. The corresponding density parameter are $\Omega_{de} = 1$, $\Omega_m = 0$ and $\Omega_r = 0$. The eigenvalues for corresponding to the critical point shows positive and negative signature are given below. The critical point shows unstable saddle behaviour.

$$\left\{ \frac{3}{2}, \frac{3}{2}, -1 \right\}.$$

- **Curve of Critical Points $C_1(x, 1-x, 0)$:** At this point, $\Omega_{de} = 1$, $\Omega_m = 0$ and $\Omega_r = 0$, i.e the Universe shows dark energy dominated phase. The accelerated dark energy dominated Universe is confirmed by the corresponding value of the EoS parameter ($\omega_{eff} = -1$) and value of the deceleration parameter ($q = -1$). Jacobian matrices with critical points have negative real parts and zero eigenvalues. This critical point, shows stable node behaviour. The corresponding eigen values are given below:

$$\{-4, -3, 0\}.$$

From the phase portrait of (FIG.- 5), we can see that the critical point A_1 is unstable node, where as curve $[(x, 1-x, 0)]$ is stable node. The B_1 is unstable saddle point. FIG.- 5 (Left Panel) describes the trajectories for critical points, where A_1 is the repeller, so it repels every trajectory and C_1 is the attractor, so it absorbs every trajectory coming towards it. The B_1 is saddle therefore, it absorbs the trajectories coming from A_1 and repel the trajectories originated from itself. FIG.- 5 (Right Panel) plane, it is important to mentioned that the system is stable not at the single point but it is stable on the curve $[(x, 1-x, 0)]$. Also, the evolution plot for Model-I given in FIG.- 6. The present value from evolution curve for the effective EoS parameter is -0.5319 and the value which is obtained using scale factor is -0.7013 . Hence from both the values, one can say that the Universe shows the quintessence behaviour. At present the density parameter for dark energy and matter gives the value ≈ 0.7 and ≈ 0.3 respectively.

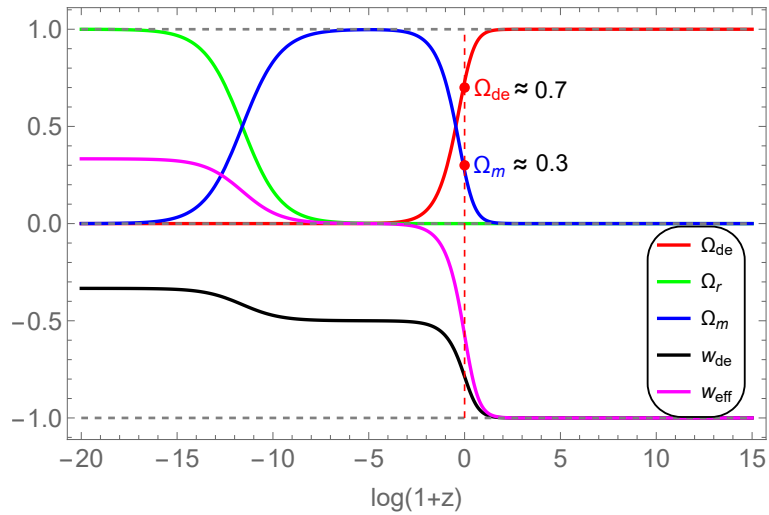


FIG. 6. Evolution of parameters for Model-I. The initial conditions: $x = 10^{-15}$, $y = 10^{-6}$ and $\sigma = 10^{-1}$. The vertical dashed red line denotes the present time.

For, $f(Q) = Qe^{\frac{\mu\lambda_2}{Q}} - Q$ [Model-II], we can get the system of differential equations as,

$$x' = \frac{(3 - 3x - 3y + \sigma)(2x + y)}{2 - y + 4(x + 1)[\ln(x + 1)]^2}, \quad (31)$$

$$y' = \frac{4(x + 1)(3 - 3x - 3y + \sigma)[\ln(x + 1)]^2}{2 - y + 4(x + 1)[\ln(x + 1)]^2}, \quad (32)$$

$$\sigma' = 2\sigma \left[\frac{3 - 3x - 3y + \sigma}{2 - y + 4(x + 1)[\ln(x + 1)]^2} - 2 \right]. \quad (33)$$

On a similar note, we can obtain the EoS parameters as,

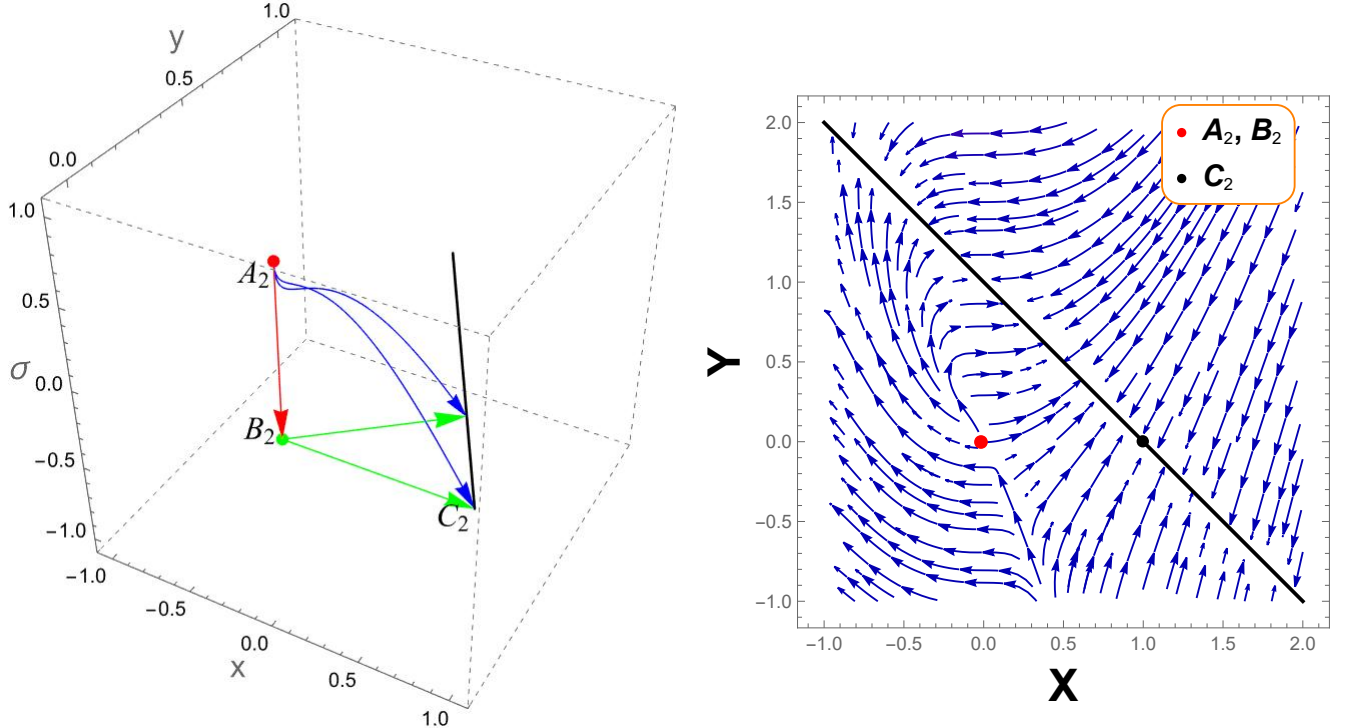
$$\omega_{eff} = -1 + \frac{6(x + y - 1) - 2\sigma}{3(2 - y + 4(x + 1)[\ln(x + 1)]^2)},$$

$$\omega_{de} = \frac{-4(\sigma + 3)[\ln(x + 1)]^2 - 2x(6[\ln(x + 1)]^2(x + 1) + 2\sigma[\ln(x + 1)]^2 + 3) + y(\sigma - 3)}{3(x + y)(2 - y + 4(x + 1)[\ln(x + 1)]^2)}.$$

Name	Point/Curve	Ω_m	Ω_r	Ω_{de}	q	ω_{eff}	ω_{de}	Phase of Universe	Stability
A_2	$(0, 0, 1)$	0	1	0	1	$\frac{1}{3}$	-	Radiation dominated	Unstable
B_2	$(0, 0, 0)$	1	0	0	$\frac{1}{2}$	0	-	Matter dominated	Unstable
C_2	$(x, 1 - x, 0)$	0	0	1	-1	-1	-1	Dark energy dominated	Stable

TABLE II. Critical Points and the corresponding cosmology for Model-II

TABLE II provides the critical points and the cosmological behaviour at these points. The details description of each critical point has been narrated below. In FIG.- 7, the 2D and 3D phase portrait have been given to understand the stability of these points.

FIG. 7. Phase-space trajectories on the x - y - σ plane (Left Panel) and the portrait on the x - y plane (Right Panel) for Model-II.

- **Critical Point $A_2 (0, 0, 1)$** : The critical point leads to the decelerating phase of the Universe, since the EoS parameter and deceleration parameter corresponding to this critical point is $\omega_{eff} = \frac{1}{3}$ and $q = 1$ respectively. The corresponding density parameter are $\Omega_{de} = 0$, $\Omega_m = 0$ and $\Omega_r = 1$. The eigenvalues for corresponding to the critical points shows positive and negative signature are given below. The critical point shows unstable node behaviour.

$$\{4, 1, 0\}.$$

- **Critical Point $B_2 (0, 0, 0)$** : At this point, $\Omega_{de} = 0$, $\Omega_m = 1$ and $\Omega_r = 0$, i.e the Universe shows matter dominated phase. The decelerated matter dominated Universe is confirmed by the corresponding value of the EoS parameter ($\omega_{eff} = 0$) and deceleration parameter $q = \frac{1}{2}$. Jacobian matrices with critical points have positive, negative real parts and zero eigenvalues. This critical point, shows unstable saddle behaviour. The corresponding eigenvalues are given below:

$$\{3, -1, 0\}.$$

- **Curve of Critical Point C_2 ($x, 1-x, 0$)** : The corresponding EoS parameter is $\omega_{eff} = -1$ and deceleration parameter is $q = -1$. This behaviour of the critical point leads to the accelerating phase of the Universe. Also, density parameters are $\Omega_{de} = 1$, $\Omega_m = 0$ and $\Omega_r = 0$. This critical point is astable node because it contains positive real part and zero eigenvalues of the Jacobian matrix.

$$\{0, -4, -3\}.$$

The phase portrait, which shows comparable trajectory plots, is an important tool in the study of dynamical systems. The stability of the models can be tested using the phase portrait. The phase portrait for system given in Eqns. (28)-(30) is shown in FIG.- 7. The (Left Panel) shows the trajectories in $x-y-\sigma$ ($3-D$) plane and (right panel) shows the trajectories in $x-y$ ($2-D$) plane. In the $3-D$ portrait, we can see that C_2 is the attractor whereas A_2 is the repeller. Here behaviour of B_2 is saddle. Every trajectory is attracted to C_2 . Similarly to Model-I, the Model-II also shows stability on the curve $[(x, 1-x, 0)]$. One can see evolution plot given in FIG.- 8 that at present time the $\omega_{eff} = -0.8625$ and FIG.- 4 (right panel) gives $\omega_{eff} = -0.8024$, which shows that the Universe goes under the quintessence phase and in late time it converges to Λ CDM.

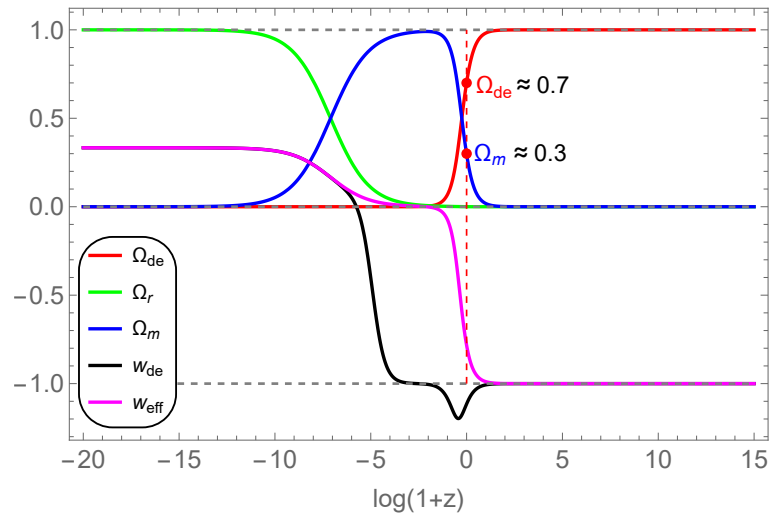


FIG. 8. Evolution of parameters for Model-II with initial conditions $x = 10^{-15}$, $y = 10^{-6}$ and $\sigma = 10^{-1}$. The vertical dashed red line denotes the present time.

V. CONCLUSION

To frame the cosmological models that concurs with the recent development of modern cosmology, several modified theories of gravity have been proposed. One among them is the symmetric teleparallel gravity or $f(Q)$ gravity. Two cosmological models are presented in this paper with some functional form of $f(Q)$ such as, (i) log-square-root model $\left[nQ_0\sqrt{\frac{Q}{\lambda_1 Q_0}} \ln \frac{\lambda_1 Q_0}{Q}\right]$ and (ii) exponential model $\left[Qe^{\frac{\mu\lambda_2}{Q}} - Q\right]$. In Model-I, both $\frac{f(Q)}{H_0^2}$ and $f_Q(Q)$ decreases gradually whereas for Model-II, $\frac{f(Q)}{H_0^2}$ increases and $f_Q(Q)$ decreases at late time. To analyse the dynamics of the Universe, we choose a time varying deceleration parameter that shows the early time deceleration and late time acceleration. Both the models are showing quintessence behaviour at present time and behaves like the Λ CDM in late time. The Model-I and Model-II presented here exhibits the value of the effective EoS parameter as $\omega_{eff} = -0.7013$ and $\omega_{eff} = -0.8024$ respectively.

The dynamical systems analysis has been performed for both the cosmological models obtained with the form of $f(Q)$ and the time varying deceleration parameter. For Model-I, the critical points/curve are $A_1 (0, 0, 1)$, $B_1 (0, 0, 0)$ and $C_1 (x, 1-x, 0)$ given in Table-I. The point A_1 is unstable node with all eigenvalues for Jacobian matrix positive

real part and B_1 is unstable saddle with positive, negative real part and zero eigenvalues for Jacobian matrix. The curve C_1 has all eigenvalues for Jacobian matrix are negative real part and zero gives us the stable node behaviour. For more idea about the critical point, the $2 - D$ phase portrait has been shown in FIG.- 5 (Right Panel). Similarly for Model-II, the critical points/curve are $A_2 (0, 0, 1)$, $B_2 (0, 0, 0)$ and $C_2 (x, 1 - x, 0)$ given in Table-I. Here also, A_2 and B_2 are unstable points respectively shows the node and saddle behaviour. While C_2 gives the stable node behaviour for Model-II. From FIG.- 6 and FIG.- 8, we can see that at present time the evolution plot gives effective EoS values for Log-square-root model and Exponential models as $\omega_{eff} = -0.5319$ and $\omega_{eff} = -0.8625$ respectively. Also at present both the models showing quintessence behaviour and converges to Λ CDM in late time. The FIG.- 6 describes the evolutionary behavior of the Universe for Model-I. At present Universe shows $\Omega_{de} \approx 0.7$ and $\Omega_m \approx 0.3$. For Model-II the FIG.- 8 shows the present values as $\Omega_{de} \approx 0.7$ and $\Omega_m \approx 0.3$. Both the models shows early radiation era and late time dark energy era, transition through matter dominated era. One can see from effective EoS parameter obtained from hybrid scale factor and effective EoS parameter from the evolution plot shows same behavior of Universe for both the models.

Finally, we would like to mention here that the non-metricity gravity can be used to obtain stable cosmological models and can able to describe the late time cosmic acceleration of the universe. According to theory, the value of EoS parameter has been important in addressing the evolution history of Universe. Scale factor and model parameters have been used in both models to constrain how well the dynamical parameters will behave. The stability of the models are analysed using the dynamical system and we get the stable points/curve for both the models.

REFERENCES

- [1] A. Addazi et al., *Progress in Particle and Nuclear Physics*, **125**, 103948 (2022).
- [2] E. Abdalla et al., *Journal of High Energy Astrophysics*, **34**, 49 (2022).
- [3] J. Martin, *Comptes Rendus Physique*, **13**, 6 (2012).
- [4] W.L. Freedman, *Nature Astronomy*, **1**, 0121 (2017).
- [5] E. Lusso et al., *Astronomy & Astrophysics*, **628**, L4 (2017).
- [6] W. Lin et al., *The Astrophysical Journal Letters*, **904**, L22 (2020).
- [7] L. Perivolaropoulos and F. Skara, *New Astronomy Reviews*, **95**, 101659 (2022).
- [8] A.G Riess et al., *The Astronomical Journal*, **116**, 3 (1998).
- [9] S. Perlmutter et al., *The Astrophysical Journal*, **517**, 2 (1999).
- [10] R. Aldrovandi and J.G. Pereira, *Teleparallel Gravity*, (2013).
- [11] J.M. Nester and H-J Yo, *arXiv:gr-qc/9809049*, (1998).
- [12] J.B. Jimenez et al., *universe*, **5**, 5070173 (2019).
- [13] B. Altschul et al., *Advances in Space Research*, **55**, 1 (2015).
- [14] J.B. Jimenez et al., *Physical Review D*, **98**, 044048 (2018).
- [15] E.D. Valentino et al., *Classical and Quantum Gravity*, **38**, 15 (2021).
- [16] W. Yang et al., *Journal of Cosmology and Astroparticle Physics*, **10**, 008 (2021).
- [17] E.D. Valentino et al., *Astroparticle Physics*, **131**, 102606 (2021).
- [18] E.D. Valentino et al., *Astroparticle Physics*, **131**, 102604 (2021).
- [19] W. Yang et al., *Physical Review D*, **101**, 083509 (2020).
- [20] I. Soudi et al., *Physical Review D* **100**, 044008 (2019).
- [21] T. Harko et al., *Physical Review D* **98**, 084043 (2018).
- [22] R. Lazkoz et al., *Physical Review D* **100**, 104027 (2019).
- [23] I. Ayuso et al., *Physical Review D*, **103**, 063505 (2021).
- [24] S.A. Narawade et al. and B. Mishra, *arXiv:2211.09701*, (2021)
- [25] S.A. Narawade et al., *Physics of the Dark Universe*, **36**, 101020 (2022).
- [26] S.K. Maurya et al., *Progress of Physics*, **70**, 2200061 (2022).
- [27] F.K. Anagnostopoulos et al., *Physics Letters B*, **822**, 136634 (2021).
- [28] L. Atayde et al., *Physical Review D*, **104**, 064052 (2021).
- [29] N. Frusciante, *Physical Review D*, **103**, 044021 (2021).
- [30] F.K. Anagnostopoulos et al., *European Physics Journal C*, **83**, 58 (2023).

- [31] M. Koussour et al., *International Journal of Modern Physics D*, **31**, 2250115 (2022).
- [32] W. Khyllep et al., *Physical Review D*, **107**, 044022 (2023).
- [33] A. Bonanno and S. Carloni, *New Journal of Physics*, **14**, 025008 (2012).
- [34] W. Khyllep et al., *Physical Review D*, **103**, 103521 (2021).
- [35] A.S Agrawal et al., *arXiv:2212.10272*, (2022).
- [36] L.K. Duchaniya et al., *European Physics Journal C*, **83**, 27 (2022).
- [37] A. Samaddar and S.S. Singh, *arXiv:2211.07376*, (2022).
- [38] L.K. Duchaniya et al., *arXiv:2302.07132*, (2022).
- [39] A. Samaddar et al., *arXiv:2302.02999*, (2023).
- [40] L. Pati et al., *arXiv:2206.11928*, (2023).
- [41] F. W. Hehl et al., *Physics Reports*, **258**, 1 (1995).
- [42] T. Ortin, Gravity and Strings, Cambridge University Press, Cambridge, England, (2015).
- [43] E.D. Valentino et al., *Physics Letters B*, **761**, 242 (2016).
- [44] S. Vagnozzi, *Physical Review D*, **102**, 023518 (2020).
- [45] R. Amanullah et al., *The Astrophysical Journal*, **716**, 712 (2010).
- [46] G. Hinshaw, et al., *The Astrophysical Journal Supplement Series*, **208**, 19 (2013).
- [47] N. Aghanim et al., *Astronomy & Astrophysics*, **A1**, 641 (2020).
- [48] E.D. Valentino et al., *entropy*, **23**, 4 (2021).
- [49] S.K. Tripathy and B.Mishra, *Modern Physics Letters A*, **30**, 1550175 (2015).
- [50] B. Mishra et al., *Modern Physics Letters A*, **33**, 1850052 (2018).
- [51] B. Mishra et al., *The European Physical Journal C*, **79**, 34 (2019).
- [52] S.K. Tripathy et al., *International Journal of Modern Physics D*, **30**, 2140005 (2021).
- [53] F.K. Anagnostopoulos et al., *European Physics Journal C*, **83**, 58 (2022).
- [54] S. Bahamonde et al., *Physics Reports*, **775**, 1 (2018).
- [55] R. D'Agostino and O. Luongo, *Physical Review D*, **98**, 124013 (2018).